The Role of Excited Rydberg States in Electron Transfer Dissociation

Monika Sobczyk and Jack Simons*

Chemistry Department and Henry Eyring Center for Theoretical Chemistry, University of Utah, Salt Lake City, Utah 84112

Received: January 23, 2006; In Final Form: February 24, 2006

Ab initio electronic structure methods are used to estimate the cross sections for electron transfer from donor anions having electron binding energies ranging from 0.001 to 0.6 eV to each of three sites in a model disulfide-linked molecular cation. The three sites are (1) the S−S σ^* orbital to which electron attachment is rendered exothermic by Coulomb stabilization from the nearby positive site, (2) the ground Rydberg orbital of the $-NH_3^+$ site, and (3) excited Rydberg orbitals of the same $-NH_3^+$ site. It is found that attachment to the ground Rydberg orbital has a somewhat higher cross section than attachment to either the σ^* orbital or the excited Rydberg orbital. However, it is through attachment either to the σ^* orbital or to certain excited Rydberg orbitals that cleavage of the S−S bond is most likely to occur. Attachment to the σ^* orbital causes prompt cleavage because the σ^* energy surface is repulsive (except at very long range). Attachment to the ground or excited Rydberg state causes the S−S bond to rupture only once a through-bond electron transfer from the Rydberg orbital to the S−S σ^* orbital takes place. For the ground Rydberg state, this transfer requires surmounting an ∼0.4 eV barrier that renders the S−S bond cleavage rate slow. However, for the excited Rydberg state, the intramolecular electron transfer has a much smaller barrier and is prompt.

I. Introduction and Background

In electron capture dissociation[1] (ECD) or electron transfer dissociation[2] (ETD) mass spectroscopy experiments, electrons are believed to first attach (primarily) to positively charged sites within the gas-phase sample to form what is called a hypervalent or Rydberg radical center. The positive sites in peptides and proteins include, for example, protonated amine or guanidinium groups on side chains as well as protonated amide units along the backbone. When a side-chain positive group is proximal to (e.g., as when involved in hydrogen bonding) either the oxygen atom of an amide unit or a disulfide bond, the nascent Rydberg radical formed when an electron attaches can subsequently induce an H atom migration to either the carbonyl oxygen or a disulfide sulfur atom to eventually generate N−C_α or S−S bond cleavage, as illustrated in the clockwise branches of Schemes 1 and 2. These very specific cleavages characterize ECD and ETD and are one of these methods' strongest attributes.

In these schemes, we show the electron being transferred from a methyl anion, which would be appropriate for the case of electron transfer dissociation (ETD) which forms the focus of the present paper. In ECD experiments, it is free electrons that attach to the positively charged sample.

In two earlier studies,[3,4] we investigated alternative pathways by which such S−S or N−C_α bonds could be cleaved in ETD or ECD. The experimental evidence that suggested alternative mechanisms might be operative is detailed in refs 3 and 4 but will not be discussed here. Following our studies[5−8] of how proximal positive charges can render exothermic direct electron attachment to low-lying antibonding orbitals, we considered in refs 3 and 4 the possibility of electron transfer (or capture) directly into a S−S σ^* or amide OCN π^* orbital. Of course, it is known[9] that direct attachment to either of these orbitals in the absence of any stabilizing Coulomb effects is endothermic (by ∼1.0 eV for the S−S σ^* and ∼2.5 eV for the amide π^*). However, we showed the presence of any nearby positively charged group (e.g., a $-NH_3^+$ unit or a sodiated analogue $-NH_2Na^+$) can differentially stabilize the electron attached state by an amount of 14.4 (eV)/R (Å) that can be estimated by

SCHEME 1

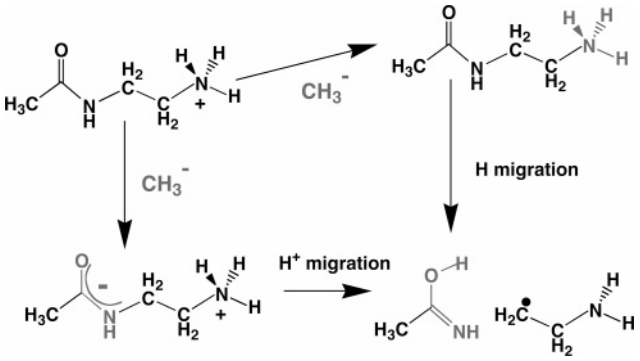

SCHEME 2

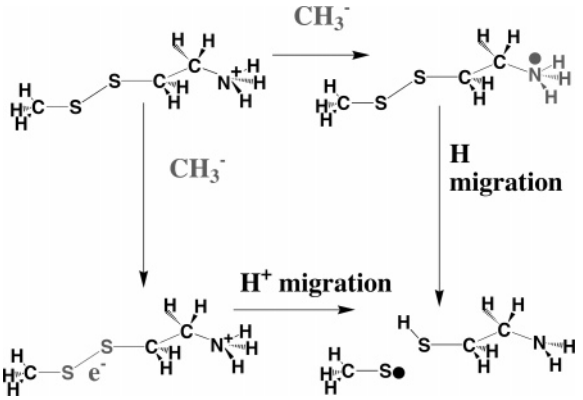

* Corresponding author. E-mail: simons@chem.utah.edu. Home page: http://simons.hec.utah.edu.

10.1021/jp0604701 CCC: $33.50
Published on Web 03/22/2006

knowing the distance (R) from the S−S or amide bond to the positive site. One result of these studies was the suggestion, also illustrated in Schemes 1 and 2, that direct electron transfer to the bond site could effect S−S or N−C_α bond cleavage, and subsequent proton migration would then lead to the same fragments as those produced by the conventional H atom migration mechanism. A similar suggestion was put forth at about the same time in ref 1j by the Turecek group. Of course, this suggestion then raises the issue of whether the electron transfer is more likely to occur to the $-NH_3^+$ Rydberg site, which provides a more exothermic channel, or to the Coulomb-stabilized bond site (i.e., to either the S−S σ^* or OCN amide π^* orbital).

Thus, the second component of our earlier studies[3,4] has been the estimation, using Landau−Zener (LZ) theory, of the rates at which electrons would be transferred from a donor anion to either the Rydberg site or to the σ^* or π^* bond site. In these studies, the two model cations shown in Schemes 1 and 2 were allowed to collide with a methyl anion. We chose the methyl anion both because its small size made the electronic structure calculations computationally feasible and because the highly localized nature of its lone-pair site of negative charge allowed us to accurately specify the distance between the donor's negative and cation's positive charges. Knowing this distance is important in implementing the LZ theory estimates for electron transfer. It should also be mentioned that the distance between the nitrogen atom of the $-NH_3^+$ unit and the midpoint of the S−S or C═O bond of our model cation was held fixed in refs 3 and 4 because we wanted to keep the Coulomb stabilization of the S−S σ^* or OCN π^* orbital constant.

In the case of S−S bond cleavage, the approach we employed to calculate electron transfer rates involved (for our N−C_α bond cleavage study, an analogous process was followed):

(1) Computing the Born−Oppenheimer potential surfaces, as functions of the methyl-carbon-to-amine-nitrogen distance, of three diabatic (meaning with specified and fixed orbital occupation) electronic states:

(a) the state in which $H_3C-S-S-CH_2-CH_2-NH_3^+$ and $^-CH_3$ interact with the "extra" electron in the methyl anion's lone-pair orbital,

(b) the state in which an electron has been transferred from the methyl anion to the (Coulomb-stabilized) S−S σ^* orbital, and

(c) the state in which an electron has been transferred from the methyl anion to the $-NH_3^+$ site's lowest Rydberg orbital.

(2) Evaluating the electronic coupling matrix elements ($H_{1,2}$) connecting pairs of these three states that undergo avoided crossings at various nitrogen−carbon distances (R). These couplings are determined from the splitting between the two adiabatic states that arise as the pairs of diabatic states interact.

(3) Using LZ theory to express the cross section (σ) for each electron transfer process in terms of the $H_{1,2}$ elements and quantities that characterize the intersecting diabatic surfaces, as we illustrate below.

In Figure 1, we show qualitatively how the three Born−Oppenheimer surfaces discussed above vary along the methyl-carbon-to- $-NH_3^+$-nitrogen distance (R_N). The ion-pair surface, relating to $H_3C-S-S-CH_2-CH_2-NH_3^+ + {}^-CH_3$, varies in the attractive Coulomb manner $-Ze^2/R_N$, while the two charge-neutralized states are relatively flat, at least at large R_N. Of course, the latter two states lie below the ion-pair state at large R_N by energy defect amounts (Δ) that depend on the electron binding energies of the methyl anion and of the S−S σ^* and

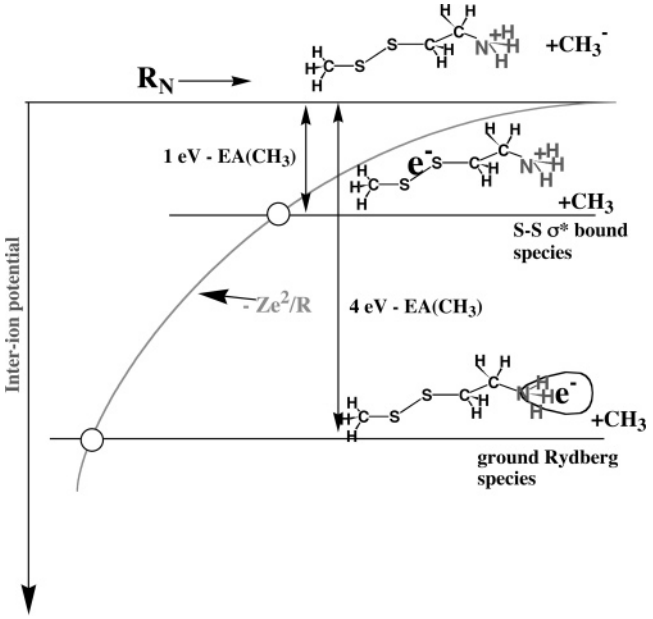

Figure 1. Potential energy of interaction between the $CH_3SSCH_2CH_2NH_3^+$ cation and the methyl anion as well as the potentials for the two charge-exchanged species.

$-NH_3^+$ sites, the latter of which are ~1 and 4 eV, respectively, at the equilibrium S−S bond length.

The essential ingredients for implementing the LZ method are the following:

(1) The critical distance (R_C) at which two diabatic curves cross. This distance can be estimated (in our ab initio calculations, we actually located the distance by finding the avoided crossing, as we show later) by solving

$$-Ze^2/R_C = -\Delta = -(\text{binding energy of the S}-\text{S or } -NH_3^+ \text{ site}) + \text{EA}(CH_3) \quad (1)$$

to obtain

$$R_C = Ze^2/\Delta = 14.4Z/\Delta \quad (2)$$

with the latter result applying when Δ is expressed in electron-volts and R is then obtained in angstroms. In this analysis, we retain the possibility of treating multiply charged positive sites by including the positive charge magnitude (Z) in our expressions, although, of course, $Z = 1$ for the model compounds discussed above.

(2) The relative speed (v) with which the anion and cation are moving (along the R_N direction) as they undergo the crossing at R_C. This speed can be estimated, assuming that most of their relative kinetic energy derives from the decrease in potential energy (Δ) as they are accelerated along the attractive Coulomb potential[10] until they reach the crossing as

$$v = (2\Delta/\mu)^{1/2} \quad (3)$$

where μ is the reduced mass of the anion−cation collision pair.

(3) The magnitude of the slope difference (δF) for the two diabatic curves as they cross at R_C. Within the approximation that one of the curves is Coulombic and the other is flat, this factor can be expressed as

$$\delta F = Ze^2/R_C^2 = \Delta^2/(14.4Z) \quad (4)$$

The LZ theory then gives the probability (P) for undergoing a transition in which the electron hops from the methyl anion to either the S−S σ^* or $-NH_3^+$ Rydberg orbital as follows

$$P = 1 - \exp[-2\pi H_{1,2}^2/(\hbar v \delta F)] \quad (5)$$

Within the so-called weak-coupling limit, in which $H_{1,2}$ is very small, which we will show later applies to the cases considered here, these probabilities can be approximated by

$$P = 2\pi H_{1,2}^2/(\hbar v \delta F) \quad (6)$$

which, in turn, can be rewritten in terms of the energy defects (Δ) as

$$P = (2\pi/\hbar) H_{1,2}^2 (\mu/2)^{1/2} 14.4Z/\Delta^{2.5} \quad (7)$$

Equation 7 allows one to see how strongly the electron transfer probabilities depend on the energy defect (Δ) and on the electronic couplings. It also suggests how these probabilities should scale with the charge (Z) of the cation. Finally, the above probability expression applies to an event in which the collision begins in the ion-pair state $H_3C-S-S-CH_2-CH_2-NH_3^+ + {}^-CH_3$ and undergoes a transition to one of the charge-neutralized states $H_3C-S-S-CH_2-CH_2-NH_3 + CH_3$ during the entrance channel of the collision. However, to compute the overall probability for starting the collision as $H_3C-S-S-CH_2-CH_2-NH_3^+ + {}^-CH_3$ and ending up (on the exit channel of the collision) as $H_3C-S-S-CH_2-CH_2-NH_3 + CH_3$, one has to consider two paths by which the overall charge state changes:

(1) $H_3C-S-S-CH_2-CH_2-NH_3^+ + {}^-CH_3$ undergoes a transition to a charge-neutralized state with probability P in the entrance channel (i.e., when moving downhill on the attractive Coulomb potential). The charge-neutralized species then evolves to smaller R-values and experiences repulsive forces that cause the two species to reverse their relative motions. Subsequently, as the charge-neutralized species move outward to larger R, they remain on the neutral state's surface (with probability $1 - P$) to ultimately generate $H_3C-S-S-CH_2-CH_2-NH_3 + CH_3$ as separated products. The overall probability for this path is $P(1 - P)$.

(2) $H_3C-S-S-CH_2-CH_2-NH_3^+ + {}^-CH_3$ does not undergo a transition to the charge-neutralized state (with probability $1 - P$) on the entrance channel but evolves to smaller R, experiences repulsive forces, and reverses direction. Upon moving outward on the Coulombic potential, this ion-pair species undergoes a transition to the charge-neutralized state with probability P to ultimately generate $H_3C-S-S-CH_2-CH_2-NH_3 + CH_3$. The overall probability for this path is $(1 - P)P$.

Thus, the total probability of generating charge-neutralized products is $2P(1 - P)$. Because, as noted above, the weak-coupling limit applies to the systems studied here, this total probability reduces to $2P$, with P given as in eqs 6 and 7.

In refs 3 and 4, we used eq 6 to compute probabilities for electron transfer in terms of the slope differences (δF) realized in our ab initio calculations, the relative velocities (v) obtained from molecular dynamics simulations of anion−cation collisions, and the coupling matrix elements ($H_{1,2}$) extracted from the two adiabatic curves associated with each crossing, as we now illustrate. Our dynamics simulations showed that, regardless of what impact parameter or relative orientation the $H_3C-S-S-CH_2-CH_2-NH_3^+ + {}^-CH_3$ collisions started with, when the trajectories reached the regions where the diabatic curves cross, the two ions' relative velocity was primarily along the methyl-carbon-to-cation-nitrogen direction. It is for this reason that we focus on this C−N distance when discussing the potential curves.

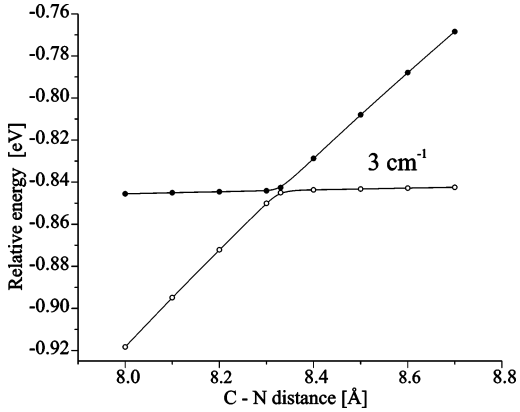

Figure 2. Energies of the $CH_3SSCH_2CH_2NH_3^+ + CH_3$ (higher curve at large R and lower curve at small R) and S−S σ^* (lower at large R and higher at small R) $CH_3SSCH_2CH_2NH_3 + CH_3$ surfaces as functions of the methyl-carbon-to- $-NH_3^+$-nitrogen distance.

Above, we explained how we use LZ theory to estimate the probabilities for electron transfer, but we still have to explain how we obtain the electronic coupling matrix element ($H_{1,2}$). In Figure 2, we show portions of the ion-pair and S−S σ^* attached Born−Oppenheimer surfaces in the region where these two diabatic surfaces undergo an avoided crossing. We take $H_{1,2}$ to be one-half of the energy splitting between the two adiabatic curves at their location (this defines R_C) of closest approach (3 cm^{-1} for the example shown in Figure 2).

When studying the electron transfer from methyl anion to the amide group of the model peptide $H_3C-(C{=}O)NH-CH_2-CH_2-NH_3^+$, we examined the splitting between two analogous curves to obtain the $H_{1,2}$ values for this case.

Finally, in refs 3 and 4, we were able to compute the cross sections[11] for electron transfer to either bond site by multiplying the probability $2P$ for electron transfer to that site by the factor πR_C^2:

$$\sigma = 4\pi^2 R_C^2 H_{1,2}^2/(\hbar v \delta F) = (4\pi^2/\hbar) H_{1,2}^2 (\mu/2)^{1/2} (14.4Z)^3/\Delta^{4.5} \quad (8)$$

It is then possible to estimate the rates of electron transfer to each of the three cation sites by multiplying the corresponding cross section by the cation−anion collision frequency (f), which, of course, depends on the ion concentration and the temperature.

From the latter form of eq 8, it is clear that the relative rates of electron transfer to the σ^* (or π^*) and $-NH_3^+$ Rydberg sites depend on two competing factors: (1) The energy defect dependence ($\Delta^{-4.5}$) favors transfer to the σ^* or π^* sites, but (2) the coupling matrix element factor ($H_{1,2}^2$) favors transfer to the ground Rydberg site (because the overlap of the methyl anion's lone-pair orbital is larger with this orbital than with either the σ^* or π^* orbitals).

In our earlier works, we were able to determine the $H_{1,2}$ and Δ factors for the various transfer events and to conclude the following:

(1) The cross sections for attachment to the σ^* or π^* bond sites are at least an order of magnitude smaller than those for attachment to the ground Rydberg site.

(2) The $H_{1,2}$ couplings are sufficiently small (a few to ~100 cm^{-1}) in all cases (i.e., σ^*, π^*, and Rydberg) to make the factor $2\pi H_{1,2}^2/(\hbar v \delta F)$ much less than unity, so the weak-coupling limit can be applied within the LZ theory.

The remainder of this paper is organized as follows. In section II, we briefly outline our strategy for designing a series of calculations that allow us to consider (1) the relative rates of electron transfer to σ^* (we will deal with transfer to amide π^* orbitals in a future paper), ground Rydberg, and excited Rydberg orbitals, (2) how these rates depend on the electron binding energy of the donor anion, and (3) at what rate the S−S bond is cleaved after electron transfer to each of the above three orbitals. In section III, we describe the theoretical methods used, and in section IV, we present and discuss the relevance of our findings.

II. Extension to Include Excited Rydberg States

In the two earlier papers,[3,4] we considered only two possible electron transfer events—transfer to the ground Rydberg orbital of the $-NH_3^+$ site or transfer to either the S−S σ^* or amide OCN π^* orbital. It is known from dissociative recombination experiments[12] that when free electrons attach to cations, they most likely attach to higher-lying Rydberg states after which a cascade of radiationless or radiative relaxations to lower Rydberg states occurs. As our earlier work demonstrated, the character of the charge-neutralized species' potential energy surface along the S−S bond coordinate differs drastically for the S−S σ^* and $-NH_3^+$ ground Rydberg attached states; the former directly dissociates, whereas the latter has a substantial barrier to S−S bond cleavage. Therefore, in the present work, we decided to explore the possibility that electron transfer to excited Rydberg states (i.e., higher Rydberg orbitals of the $-NH_3^+$ site) would be competitive with transfer to the ground Rydberg site. We also decided to explore how the fate of the nascent charge-neutralized species (e.g., $H_3C-S-S-CH_2-CH_2-NH_3$) would depend on whether transfer occurred to the ground or excited Rydberg state. In particular, we wanted to determine the barriers to S−S bond rupture for the excited Rydberg states and to compare these barriers to the substantial barrier we found for the ground Rydberg state.

Finally, to extend our studies in an additional dimension, we decided to carry out all of the evaluations of cross sections for electron transfer to σ^*, ground Rydberg, and excited Rydberg orbitals for anions having a range of electron binding energies. To accomplish this while not varying other characteristics of the anion donor, we used a "trick" in which we modified the methyl anion's electron binding energy by artificially modifying the nuclear charge (by fractional amounts) on its carbon atom; smaller nuclear charges lead to smaller binding energies. As a result, we were able to treat electron transfer from a donor anion having a binding energy of 0.001, 0.2, 0.4, or 0.6 eV.

III. Methods

The internal structure (bond lengths and angles) of the parent $H_3C-S-S-CH_2-CH_2-NH_3^+$ cation was first optimized at the Hartree−Fock (HF) self-consistent field (SCF) level and subsequently held fixed throughout our calculations characterizing the collisions with the $^-CH_3$ anion. We froze the internal geometry of this cation because we are attempting to model the environment within a peptide or protein in which a S−S σ^* orbital is Coulomb stabilized by a positively charged site whose location remains quite fixed.

To properly describe the ground and excited Rydberg states of the $R-NH_3$ species, we added to the aug-cc-pVDZ basis sets[13] an additional set (1s1p) of extra diffuse functions[14] centered on the nitrogen atom. This kind of basis was shown earlier[14] to be capable of reproducing the energies of such low Rydberg states of nitrogen-centered radicals.

To generate the four energy surfaces ($H_3C-S-S-CH_2-CH_2-NH_3^+ + {}^-CH_3$, $H_3C-S-S-CH_2-CH_2-NH_3$ ground Rydberg + CH_3, $H_3C-S-S-CH_2-CH_2-NH_3$ excited Rydberg + CH_3, and $H_3C-S-S-CH_2-CH_2-NH_3$ S−S σ^* + CH_3) needed to evaluate the cross sections for electron transfer, we performed calculations at the unrestricted HF (UHF) level. We did not proceed beyond this level because, as we show later, the $H_{1,2}$ coupling matrix elements we obtained were extremely small (<70 cm^{-1}) in all cases. Being able to determine these $H_{1,2}$ values to higher accuracy would not change the fact that they are all small and thus would not alter the conclusions drawn later, so we decided not to go beyond the SCF level in this component of our work.

In the calculations dealing with the fate of the nascent ground or excited Rydberg radical, we employed the unrestricted second-order Møller−Plesset (UMP2) method and examined the energies of the ground Rydberg, excited Rydberg, and S−S σ^* attached states as functions of the S−S bond length (with the other internal coordinates of $H_3C-S-S-CH_2-CH_2-NH_3$ held fixed for the reasons noted earlier). The use of an unrestricted method was necessary both to achieve a qualitatively correct description of the homolytic cleavage of the S−S bond and because $H_3C-S-S-CH_2-CH_2-NH_3$ is an open-shell system. We used the UMP2 method rather than the UHF approach in this case because the $H_{1,2}$ matrix elements were found to be much larger than the earlier cases discussed above, so we wanted to determine them to higher accuracy.

Because the methods we used are based on an unrestricted Hartree−Fock approach, it is important to make sure that little, if any, artificial spin contamination enters into the final wave functions. We computed the expectation value $\langle S^2 \rangle$ for species studied in this work and found values not deviating from 0.75 (after annihilation) by more than 0.03 in all open-shell doublet neutral cases.

The calculations we performed are especially problematic at distances where one or more of the $H_3C-S-S-CH_2-CH_2-NH_3 + CH_3$ states' energies lie above that of the $H_3C-S-S-CH_2-CH_2-NH_3^+ + {}^-CH_3$ ion-pair state. In such cases, great care must be taken to prevent variational collapse. For the ground Rydberg state of $H_3C-S-S-CH_2-CH_2-NH_3$, this was not an issue, but it was for the excited Rydberg state of $H_3C-S-S-CH_2-CH_2-NH_3$. For this case, we found it adequate to use the "alter" option in the Gaussian program to begin the SCF process with the desired orbital occupancy. Convergence to the desired (excited Rydberg) state was then verified by visually inspecting the singly occupied orbital after convergence.

For the state of $H_3C-S-S-CH_2-CH_2-NH_3$ in which the electron is attached to the S−S σ^* orbital, the alter option did not work (i.e., variational collapse took place), so we had to use another approach. In the method we used to overcome the problem for this state, we introduced a device that we have exploited in many past applications.[15] Specifically, we artificially increased the nuclear charges of the sulfur atoms involved in accepting the transferred electron by a small amount (δq) and carried out the UHF or UMP2 calculations with these artificial nuclear charges. By plotting the energies of the states of $H_3C-S-S-CH_2-CH_2-NH_3 + CH_3$ for several values of the charge increment (δq) and extrapolating to $\delta q = 0$, we were able to evaluate the true energy of these $H_3C-S-S-CH_2-CH_2-NH_3 + CH_3$ states. Finally, the Gaussian 03 suite of programs[16] was used to perform all of the calculations, and the Molden visualization program[17] was employed to examine the molecular orbitals.

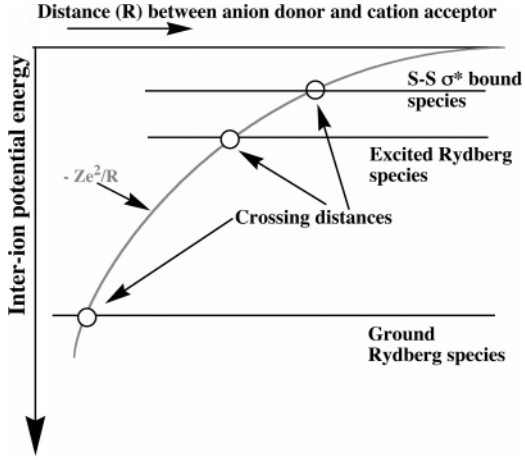

Figure 3. Qualitative depiction of the variation of the four cation−anion state energies as functions of the anion-to-nitrogen distance (*R*).

IV. Results and Discussion

As mentioned briefly earlier, we considered processes in which an electron is transferred from a modified methyl donor anion denoted A^- to any of three possible orbitals of the model disulfide-linked cation $H_3C-S-S-CH_2-CH_2-NH_3^+$ (within which we keep the distance between the nitrogen atom and the midpoint of the S−S bond fixed[18]) shown in Scheme 1. The three orbitals to which the electron can be transferred are

(1) the S−S antibonding σ^* orbital to which electron attachment has been rendered vertically exothermic by ∼2 eV by the presence of the protonated amine's Coulomb potential,

(2) an excited Rydberg orbital located on the protonated amine site for which electron attachment is also ∼2 eV exothermic, and

(3) the ground-state Rydberg orbital located on the protonated amine site for which electron attachment is ∼4 eV exothermic.

Of course, there are many excited Rydberg states that we might have considered, but only one was examined in detail for reasons that we make clear later.

The qualitative shapes of the Born−Oppenheimer electronic energies of the four states corresponding to the electron residing on the donor anion or in one of the three orbitals just discussed as functions of the anion−cation distance (*R*) are shown in Figure 3.

A. Nominal Cross Sections. Each of the three states in which an electron has transferred from A^- is shifted to lower energy than the $H_3C-S-S-CH_2-CH_2-NH_3^+\cdots A^-$ state by an amount equal to the difference (Δ) between the electron binding energy of the donor anion (EA_{anion}) and the binding energy of the S−S σ^*, excited Rydberg, or ground Rydberg site (each of which we denote EA_{site})

$$\Delta = EA_{site} - EA_{anion}$$

The critical distance (R_C) at which the descending Coulomb potential crosses the energy of any state in which the electron has been transferred is given in eq 2. We will refer to the cross section computed in terms of this critical distance

$$\sigma^\circ = \pi R_C^{\,2} = \pi(14.4Z/\Delta)^2 \qquad (9)$$

as the nominal cross section for the transfer of an electron from an anion having binding energy EA_{anion} to the site with binding energy EA_{site}. We note that the nominal cross section displays the expected quadratic scaling with charge *Z*. In Table 1, we list these nominal cross sections for cases in which the anion's electron binding energy is 0.001, 0.2, 0.4, and 0.6 eV and for electron transfer to either of the three bond sites discussed above.

TABLE 1: Nominal Cross Sections, $\sigma^\circ = \pi R^2_C$ (Å²), for Three Sites and for Four Anion Electron Binding Energies (eV)

anion binding energy (eV)	S−Sσ^*	excited Rydberg	ground Rydberg
0.001	156	114	32
0.2	171	121	33
0.4	188	128	34
0.6	218	140	36

Clearly, the S−S σ^* site's nominal cross section is largest and that of the ground Rydberg site is smallest. Moreover, these cross sections decrease as the anion's electron binding energy decreases, reflecting the inverse dependence on Δ shown in eq 9.

B. Electronic Coupling Elements. These nominal cross sections would be appropriate for describing electron transfer from A^- to the three sites mentioned above if the probability (*P*) of electron transfer when a collision between $H_3C-S-S-CH_2-CH_2-NH_3^+$ and A^- reaches R_C were unity. However, these probabilities are, as we now demonstrate, much less than unity because of the very weak coupling between the donor anion's highest occupied molecular orbital (for all values of the anion's binding energy considered here) and the cation's ground Rydberg, excited Rydberg, and S−S σ^* orbitals. To estimate the probabilities of electron transfer, we employ LZ theory, which expresses 2*P* as in eqs 6 and 7. To make use of these equations, we had to first evaluate the coupling matrix elements ($H_{1,2}$) appropriate for electron transfer to the three orbitals and for each of the four anion binding energies. The adiabatic Born−Oppenheimer curves for each of these 12 cases are shown in Figure 4 where we also give the resultant $H_{1,2}$ values in cm^{-1}.

Before moving on to discuss the results we obtained by using the $H_{1,2}$ values shown in Figure 4, we want to emphasize the following:

(1) All of the $H_{1,2}$ values are quite small (<70 cm^{-1}). As we will show below, this means that all of the electron transfer probabilities (2*P*) are much less than unity, thus justifying our use of the weak-coupling formulas discussed earlier.

(2) Because the splittings between the adiabatic curves, and hence $H_{1,2}$, are extremely small, the numerical precision in our calculations probably limits our determining these coupling elements to within a factor of 10.

(3) Especially for the ground-state Rydberg case, where the two adiabatic curves interact at small *R*-values where significant anion−cation repulsive forces are operative, the two diabatic curves are not well represented even locally by straight lines. This further limits our ability to accurately determine the $H_{1,2}$ values for this case.

As a result, we think it unwise to attempt to represent as accurate our final electron cross sections except to say that they are all much smaller than their nominal cross sections. As we noted in discussing eq 8, there are two competing factors in determining the cross sections: the energy defect which appears as $\Delta^{-4.5}$ and the coupling elements which appear as $H_{1,2}^2$. We feel confident that our analysis of the Δ-dependence is correct, but because of the major uncertainties in the $H_{1,2}$ values we extract from Figure 4, we believe it best to quote large percentage uncertainties in the cross sections and in the electron transfer rates they imply.

C. Effects of Energy Defects on Probabilities. Because of the significant uncertainties in determining the $H_{1,2}$ values, it is

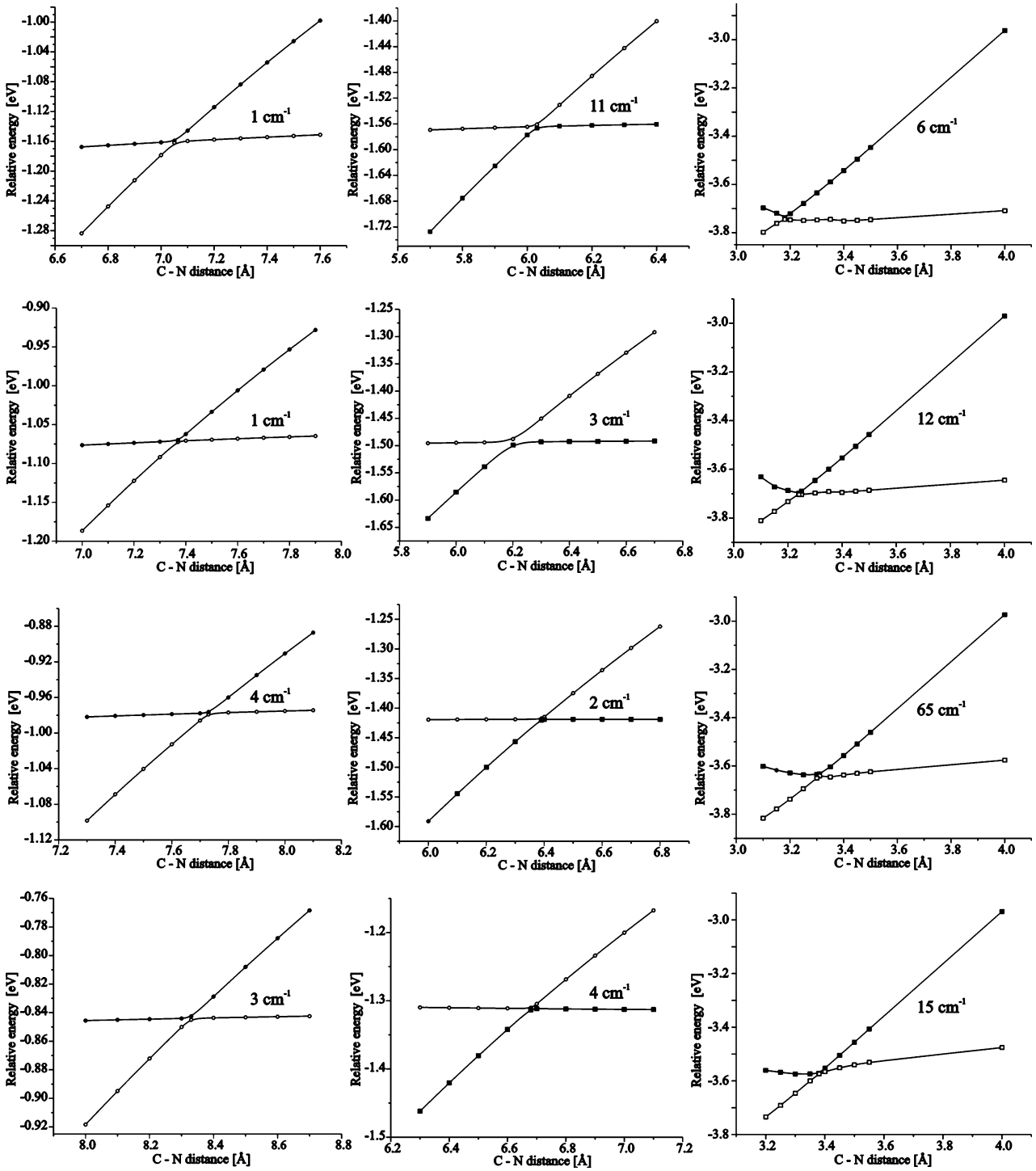

Figure 4. Adiabatic curves showing avoided crossings and $H_{1,2}$ values for (left to right) S−S σ*, excited Rydberg, and ground Rydberg orbitals and (top to bottom) for anion electron binding energies of 0.001, 0.2, 0.4, and 0.6 eV.

useful to examine separately the two contributions to the electron transfer probabilities and cross sections obtained from eq 8. Thus, in Table 2, we show the dependence of the cross sections on the energy defect factors ($\Delta^{-4.5}$), and in Table 3, we display the total probabilities ($2P$) appropriate to the three sites and four anion binding energies, respectively. Then, in Table 4, we give the full electron transfer cross sections for each of the three sites and for the four anion electron binding energies.

These data indicate that energy factors tend to favor attachment to the excited Rydberg and σ* orbitals by at least an order of magnitude over attachment to the ground Rydberg orbital. As seen from Table 1, the nominal cross section favors the excited Rydberg and S−S σ* sites. The data of Tables 1 and 2 also suggest that the nominal and total cross sections should

TABLE 2: Energy Defect Factor, $\Delta^{-4.5} = (EA_{site} - EA_{anion})^{-4.5}$ (All Values Must Be Multiplied by 10^{-2}), with Energies in eV for Three Sites and for Four Anion Electron Binding Energies

anion binding energy (eV)	σ_{SS}*	excited Rydberg	ground Rydberg
0.001	4.4	1.6	0.19
0.2	7.1	2.4	0.25
0.4	12.1	3.6	0.31
0.6	26.8	6.4	0.44

TABLE 3: Electron Transfer Probabilities, $2P = 4\pi H_{1,2}^2/(\hbar v \delta F)$ (All Must Be Multiplied by 10^{-6}), for Three Sites and for Four Anion Electron Binding Energies (eV)

anion binding energy (eV)	σ_{SS}*	excited Rydberg	ground Rydberg
0.001	14	817	45
0.2	19	64	192
0.4	222	26	6278
0.6	165	134	359

TABLE 4: Electron Transfer Cross Sections, $\sigma = 4\pi^2 R_C^2 H_{1,2}^2/(\hbar v \delta F)$ (in Units of 10^{-2} Å), for Three Sites and for Four Anion Electron Binding Energies (eV)

anion binding energy (eV)	σ_{SS}*	excited Rydberg	ground Rydberg
0.001	0.22	9.4	0.14
0.2	0.32	0.78	0.62
0.4	4.2	0.34	22
0.6	3.6	1.9	1.3

decrease as the donor anion's electron binding energy decreases. It is our belief that these trends are reliable because they do not depend on the electronic coupling elements ($H_{1,2}$) which we earlier explained contain substantial uncertainties.

D. Transfer Probabilities and Cross Sections. In contrast to what we observed in Tables 1−2, the probability and total cross-section data of Tables 3 and 4, respectively, do not display clear trends as the electron binding energy of the donor anion is varied or among the three electron binding sites. The large uncertainties in determining the $H_{1,2}$ couplings are what causes the lack of clarity in the data of Tables 3 and 4. However, although there is substantial percentage uncertainty in the $H_{1,2}$ values, there is little doubt that these coupling elements are all quite small (<70 cm^{-1}). Thus, it is safe to conclude that

(1) all of the electron transfer probabilities (as shown in Table 3) are small (<0.01) and

(2) all of the electron transfer cross sections (Table 4) are less than the nominal cross sections (Table 1) and less than 1 $Å^2$.

E. Summary for Electron Transfer Cross Sections. We believe the results of our simulations presented above can be used to reach certain conclusions:

(1) Clearly, all of the electron transfer probabilities are much less than unity, so the electron transfer events studied here occur in the weak-coupling limit in which it requires between a thousand and a million collisions before electron transfer is likely to occur.

(2) From Figure 4, we see that the coupling elements ($H_{1,2}$) are very small (1−70 cm^{-1}) for all anion binding energies and for all three bond sites. Thus, although significant uncertainties exist in their precise values, there is no doubt they are all less than 100 cm^{-1}.

(3) From Figure 4, it appears that the couplings are similar in magnitude for the S−S σ* and excited Rydberg sites and somewhat larger (a factor of 5−10) for the ground Rydberg site. The quadratic dependence of the probability and cross section on $H_{1,2}$ means that the couplings favor transfer to the ground Rydberg site by 25−100.

(4) From Table 2, we see that the energy defect factor favors transfer to the S−S σ* and excited Rydberg sites over the ground Rydberg site by a factor of 40−300.

(5) Because the total cross sections are proportional to the energy defect factor multiplied by $H_{1,2}^2$, we expect (from points 3 and 4) the total electron transfer cross sections to be similar for attachment to all three sites and to not vary much with the donor anion's binding energy. The cross sections in Table 4 are consistent with these expectations.

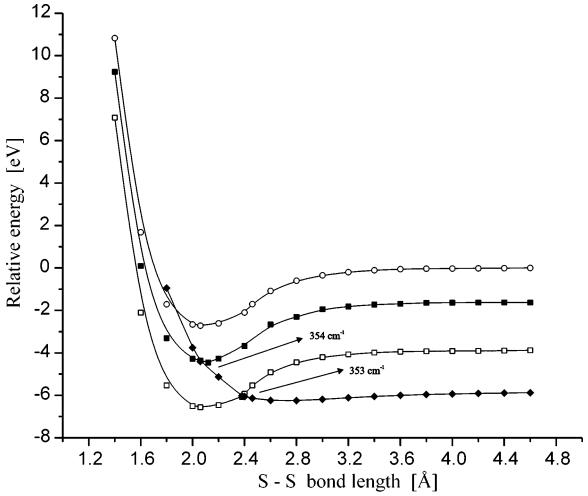

Figure 5. MP2-level energies of the parent cation (open circles) and of the species in which an electron is attached to the ground Rydberg orbital (open squares), the excited Rydberg orbital (filled squares), or the S−S σ* orbital (filled diamonds) as functions of the S−S bond length. The MP2-level $H_{1,2}$ coupling matrix elements are also shown.

F. What Happens after the Electron Transfers? Thus far, it appears that we must conclude that collisions involving donor anions having binding energies in the 0.001−0.6 eV range and the model S−S bound protonated species can lead (at similar rates) to charge neutralization in which the electron has transferred to the S−S σ* orbital, to the $-NH_3^+$ ground-state orbital, or to an excited Rydberg orbital of the $-NH_3^+$ site. Although we examined only the lowest excited Rydberg state,[19] we believe it likely that electron transfer to other Rydberg states can occur and that their attachment cross sections will be comparable to those found here. These conclusions then lead us to consider the fates of the nascent charge-neutralized states and, in particular, to determine whether they can be expected to lead to S−S bond cleavage.

To address this issue, we computed, at the MP2 level, the Born−Oppenheimer energy profiles of the S−S σ*, excited Rydberg, and ground Rydberg charge-neutralized species (in the absence of the methyl radical which is assumed to have departed once the collision has taken place) as functions of the S−S bond length. Our findings are displayed in Figure 5. In Figure 6, we show the orbitals involved in the electron transfer events.

The data shown in Figure 5 allow us to conclude the following:

(1) Direct attachment to the S−S σ* orbital leads to direct and prompt fragmentation of the S−S bond because the corresponding energy surface is repulsive except at very large *R*-values.

(2) Attachment to the ground Rydberg orbital produces a charge-neutralized species that must overcome, by stretching the S−S bond, a barrier lying ∼0.4 eV above the zero-point level to access a geometry where the ground Rydberg and S−S σ* states intersect (near 2.4 Å). At this surface intersection, the Rydberg species can evolve (with a probability that we evaluate later) into the S−S σ* species and subsequently undergo S−S bond rupture.

(3) Attachment to the excited Rydberg orbital produces a charge-neutralized species that must overcome a small barrier[20] ∼0.06 eV above the zero-point level to access an intersection with the S−S σ* state (near 2.0 Å). At this intersection, the

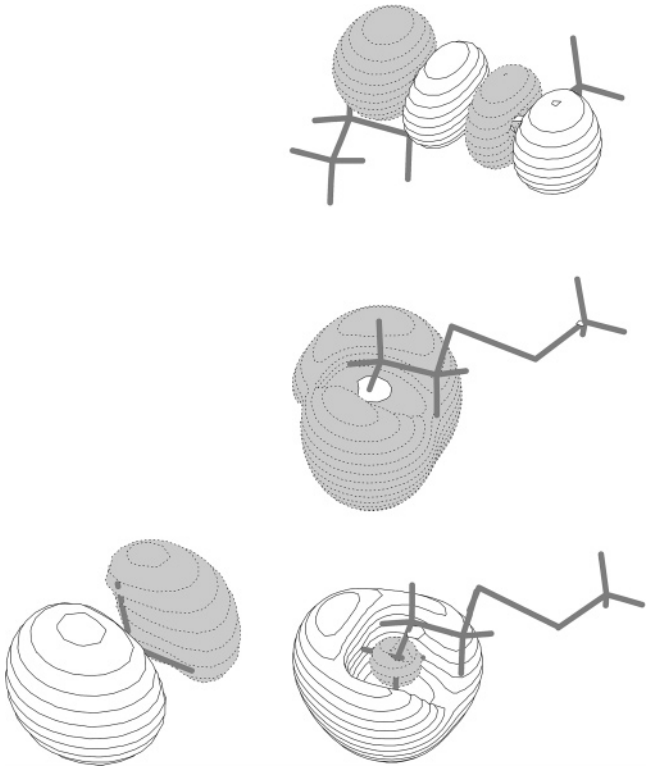

Figure 6. Orbitals involved in the electron transfer event: (right) S−S σ^* (top), excited Rydberg (middle), and ground Rydberg (bottom); (left) methyl lone pair.

excited Rydberg species can evolve (with a probability that we compute later) onto the repulsive S−S σ^* surface and fragment the S−S bond.

There are, of course, many other excited Rydberg states that we might have considered. The state upon which we focus here is not the lowest excited Rydberg state; instead, it is the lowest for which the intersection with the repulsive S−S σ^* state occurs close to the zero-point vibration of the S−S bond. Lower Rydberg states have intersections with the σ^* state that, similar to the case for the ground Rydberg state, require surmounting a larger barrier. Higher Rydberg states cross the σ^* state within the zero-point motion of the S−S bond (as can be inferred by examining how the excited Rydberg and the parent cation curves cross the σ^* state in Figure 5), so they should behave much like the excited Rydberg state we study here.

In Figure 5, we also show the MP2-level electronic coupling matrix elements ($H_{1,2}$) that pertain to the ground-Rydberg-to-σ^* (353 cm^{-1}) and excited-Rydberg-to-σ^* (354 cm^{-1}) surface interactions. When computed at the SCF level, these couplings are 778 and 850 cm^{-1}, respectively. Although the MP2 results should be more accurate, we offer these SCF data as well to give the reader some idea of the uncertainty in our estimates.

Because these (MP2 or SCF) $H_{1,2}$ values are ∼100 times larger than those discussed earlier, their evaluations were not plagued with what limited our ability to achieve accurate $H_{1,2}$ values for the anion-donor-to-cation-acceptor electron transfer. We can now make use of the couplings to compute the probabilites with which the nascent ground or excited Rydberg states undergo transitions to the repulsive S−S σ^* state. These estimates can be made by multiplying the frequency (F) with which the S−S bond is stretched (as it vibrates) to the crossing point times the probability for transitions between the two states.

The frequency (F) can be estimated by taking the vibrational frequency (ν) of the S−S bond (we computed 562 cm^{-1} which corresponds to a frequency (ν) of $\sim 2 \times 10^{13}$ s^{-1}) times the thermal probability, $p = \exp(-h\nu(\upsilon^*)/kT)/(1 - \exp(-h\nu/kT))$, that the S−S bond is in the vibrational level υ^* necessary to access the surface intersection. Of course, as is clear from Figure 5, for the excited Rydberg state, υ^* is 1, so p is high, while, for the ground Rydberg state, $\upsilon^* > 6$, so p is quite small.

The probability (P) that the ground or excited Rydberg state undergoes a through-bond electron transfer to the σ^* state if S−S vibration accesses the surface intersection can be expressed within LZ theory as in eq 5. We have to use this form of the LZ expression because we are now not in the weak-coupling regime. Using the $H_{1,2}$ values (353 and 354 cm^{-1}) shown in Figure 5 along with the corresponding slope differences (δF) and speeds (υ), we evaluate these transition probabilities and obtain

$$P_{\text{ground Rydberg}} = 0.13 \tag{10}$$

$$P_{\text{excited Rydberg}} = 0.51 \tag{11}$$

Thus, for both the ground and excited Rydberg states, the coupling to the σ^* state is strong enough to make the probability of undergoing such a transition very substantial. We should mention how the speeds (υ) needed to compute the LZ surface hopping probabilities have been estimated. We know the frequency (ν) of the S−S vibration, and for any vibrational level (υ), we can evaluate the left and right turning points for this bond's oscillatory motion. Using twice the distance between the left and right turning points times the frequency (ν), we can estimate the (average) speed at which the S−S bond is moving. Of course, this speed is a classical quantity, whereas the true S−S bond motion is governed by quantum mechanics. Moreover, this is only the average speed; the speed is higher near the midpoint of the vibration and lower near the turning points. Nevertheless, this is how we estimate υ to use in the LZ expression.

Combining these probabilities for hopping with the frequencies for accessing the surface intersections, we can evaluate the net rates at which the ground or excited Rydberg states decay into the dissociative σ^* state:

$$\text{rate}_{\text{ground Rydberg}} = 0.13(2 \times 10^{13}) \exp(-h\nu 6/kT)/(1 - \exp(-h\nu/kT)) \tag{12}$$

$$\text{rate}_{\text{excited Rydberg}} = 0.51(2 \times 10^{13}) \exp(-h\nu/kT)/(1 - \exp(-h\nu/kT)) \tag{13}$$

Using our computed harmonic S−S vibrational frequency (562 cm^{-1}) and noting that, at 300 K, kT corresponds to 0.59 kcal mol^{-1} or 208 cm^{-1}, the factor $\exp(-h\nu/kT)$ is 0.067 and $\exp(-6h\nu/kT)$ is 9×10^{-8}. Thus, the net rate of transitions from the excited Rydberg state to the σ^* state will be $\sim 10^{12}$ s^{-1} (i.e., requiring only a few vibrations of the S−S bond), while the rate of transitions from the ground Rydberg state will be many orders of magnitude smaller.

V. Conclusions

The ab initio theoretical studies whose results we presented here allow us to conclude the following:

(1) Electrons can be transferred from alkyl anions having a wide range of electron binding energies to the S−S σ^*, $-NH_3^+$ excited Rydberg, or $-NH_3^+$ ground Rydberg orbitals with similar cross sections, although the ground $-NH_3^+$ site is favored by a factor of ∼10.

(2) The transfer cross sections are at least 2 orders of magnitude smaller than the nominal cross sections (defined in eq 9), which reflects the fact that the probabilities for electron transfer to any of the orbitals in a single collision are small.

(3) The nominal electron transfer cross section scales with the charge (Z) of the sample as Z^2, whereas the total cross section scales (for these weak-coupling cases) as Z^3.

(4) The nominal and total electron transfer cross sections seem to decrease as the electron binding energy of the donor anion decreases (Tables 1 and 2). This trend may suggest what can be expected for electron capture dissociation experiments where a free electron rather than a stable anion serves as the source of the electron.

(5) After direct electron transfer to the S−S σ^* orbital, cleavage of the S−S bond is prompt.

(6) After electron transfer to the lowest Rydberg orbital, a substantial barrier (~0.4 eV) must be overcome before the electron can undergo a through-bond transfer to the S−S σ^* orbital to cleave the S−S bond. This large barrier causes this event to be very slow.

(7) After electron transfer to the excited Rydberg orbital studied here (it is the lowest orbital having a principal quantum number one higher than that of the ground state), a much smaller barrier (~0.06 eV) must be overcome before the electron can undergo a through-bond transfer to the S−S σ^* orbital to cleave the S−S bond. As a result, this event is very fast (within several vibrational periods).

Therefore, we suggest that ETD can involve the transfer of an electron to any higher Rydberg orbital of a positively charged site, followed by sequential relaxation to lower Rydberg states until a state is reached for which the S−S σ^* state's potential crosses that Rydberg state's potential within or very near to zero-point accessible bond lengths. A through-bond electron transfer can then (within a few vibrational periods) allow the electron to migrate from the Rydberg orbital to the S−S σ^* orbital and thus cleave the S−S bond.

In future studies along the lines introduced in this paper, we plan to consider

(1) N−C_α bond cleavage effected by electron transfer to excited Rydberg orbitals followed by through-bond electron transfer from the Rydberg orbital to the amide OCN π^* orbital and

(2) the distance dependence of the through-bond coupling matrix elements ($H_{1,2}$) arising in the Rydberg-to-σ^* electron transfer event so we can predict how far from a S−S bond (or an amide N−C_α bond) a protonated site can be and still effect bond cleavage through the mechanism studied here.

Acknowledgment. Support of the National Science Foundation through grant CHE 0240387 is appreciated. Significant computer time provided by the Center for High Performance Computing at the University of Utah and by the Academic Computer Center in Gdansk (TASK) is also gratefully acknowledged.

References and Notes

(1) (a) Zubarev, R. A.; Kelleher, N. L.; McLafferty, F. W. *J. Am. Chem. Soc.* **1998**, *120*, 3265. (b) Zubarev, R. A.; Kruger, N. A.; Fridriksson, E. K.; Lewis, M. A.; Horn, D. M.; Carpenter, B. K.; McLafferty, F. W. *J. Am. Chem. Soc.* **1999**, *121*, 2857. (c) Zubarev, R. A.; Horn, D. M.; Fridriksson, E. K.; Kelleher, N. L.; Kruger, N. A.; Lewis, M. A.; Carpenter, B. K.; McLafferty, F. W. *Anal. Chem.* **2000**, *72*, 563. (d) Zubarev, R. A.; Haselmann, K. F.; Budnik, B.; Kjeldsen, F.; Jensen, F. *Eur. J. Mass Spectrom.* **2002**, *8*, 337. Much of the pioneering work aimed at understanding the mechanism(s) by which ECD operates has been reported in ref 1 and by the Turecek and Uggerud groups in, for example: (e) Syrstad, E. A.; Turecek, F. *J. Phys. Chem. A* **2001**, *105*, 11144. (f) Turecek, F.; Syrstad, E. A. *J. Am. Chem. Soc.* **2003**, *125*, 3353. (g) Turecek, F.; Polasek, M, Frank, A.; Sadilek, M. *J. Am. Chem. Soc.* **2000**, *122*, 2361. (h) Syrstad, E. A.; Stephens, D. D.; Turecek, F. *J. Phys. Chem. A* **2003**, *107*, 115. (i) Turecek, F. *J. Am. Chem. Soc.* **2003**, *125*, 5954. (j) Syrstad, E. A.; Truecek, F. *J. Am. Soc. Mass. Spectrom.* **2004**, *16*, 208. (k) Uggerud, E. *Int. J. Mass. Spectrom.* **2004**, *234*, 45.

(2) (a) Syka, J. E. P.; Coon, J. J.; Schroeder, M. J.; Shabanowitz, J.; Hunt, D. F. *Proc. Natl. Acad. Sci.* **2004**, *101*, 9528. (b) Coon, J. J.; Syka, J. E. P.; Schwartz, J. C.; Shabanowitz, J.; Hunt, D. F. *Int. J. Mass Spectrom.* **2004**, *236*, 33. (c) Pitteri, S. J.; Chrisman, P. A.; McLuckey, S. A. *Anal. Chem.* **2005**, *77*, 5662. (d) Gunawardena, H. P.; He, M.; Chrisman, P. A.; Pitteri, S. J.; Hogan, J. M.; Hodges, B. D. M.; McLuckey, S. A. *J. Am. Chem. Soc.* **2005**, *127*, 12627.

(3) Anusiewicz, I.; Berdys-Kochanska, J.; Simons, J. *J. Phys. Chem. A* **2005**, *109*, 5801.

(4) Anusiewicz, I.; Berdys-Kochanska, J.; Piotr Skurski.; Simons, J. *J. Phys. Chem. A* **2006**, *110*, 1261.

(5) Sawicka, A.; Skurski, P.; Hudgins, R. R.; Simons, J. *J. Phys. Chem. B* **2003**, *107*, 13505.

(6) Sobczyk, M.; Skurski, P.; Simons, J. *Adv. Quantum Chem.* **2005**, *48*, 239.

(7) Sawicka, A.; Berdys-Kochaska, J.; Skurski, P.; Simons, J. *Int. J. Quantum Chem.* **2005**, *102*, 838.

(8) Anusiewicz, I.; Berdys, J.; Sobczyk, M.; Sawicka, A.; Skurski, P.; Simons, J. *J. Phys. Chem. A* **2005**, *109*, 250.

(9) Dezarnaud-Dandine, C.; Bournel, F.; Troncy, M.; Jones, D.; Modelli, A. *J. Phys. B: At. Mol. Opt. Phys.* **1998**, *31*, L497.

(10) The energy defects (Δ) pertinent to the species studied here are >1 eV, which greatly exceeds the thermal collision energies used in most ETD experiments, so this assumption is valid.

(11) We should note that, if the electronic couplings ($H_{1,2}$) were strong enough to make the probability (P) for electron transfer close to unity, the cross sections would be equal to πR_C^2, which in turn would reduce to $\pi(14.4Z/\Delta)^2$ and display quadratic rather than cubic dependence on the cation's charge (Z).

(12) Vejby-Christensen, L.; Andersen, L. H.; Heber, O.; Kella, D.; Pedersen, H. B.; Schmidt, H. T.; Zajfman, D. *Astrophys. J.* **1997**, *483*, 531.

(13) Kendall, R. A.; Dunning, T. H., Jr.; Harrison, R. J. *J. Chem. Phys.* **1992**, *96*, 6796.

(14) (a) Gutowski, M.; Simons, J. *J. Chem. Phys.* **1990**, *93*, 3874. (b) Skurski, P.; Gutowski, M.; Simons, J. *Int. J. Quantum Chem.* **2000**, *80*, 1024.

(15) See, for example, the description offered in ref 8.

(16) Frisch, M. J.; Trucks, G. W.; Schlegel, H. B.; Scuseria, G. E.; Robb, M. A.; Cheeseman, J. R.; Montgomery, J. A., Jr.; Vreven, T.; Kudin, K. N.; Burant, J. C.; Millam, J. M.; Iyengar, S. S.; Tomasi, J.; Barone, V.; Mennucci, B.; Cossi, M.; Scalmani, G.; Rega, N.; Petersson, G. A.; Nakatsuji, H.; Hada, M.; Ehara, M.; Toyota, K.; Fukuda, R.; Hasegawa, J.; Ishida, M.; Nakajima, T.; Honda, Y.; Kitao, O.; Nakai, H.; Klene, M.; Li, X.; Knox, J. E.; Hratchian, H. P.; Cross, J. B.; Adamo, C.; Jaramillo, J.; Gomperts, R.; Stratmann, R. E.; Yazyev, O.; Austin, A. J.; Cammi, R.; Pomelli, C.; Ochterski, J. W.; Ayala, P. Y.; Morokuma, K.; Voth, G. A.; Salvador, P.; Dannenberg, J. J.; Zakrzewski, V. G.; Dapprich, S.; Daniels, A. D.; Strain, M. C.; Farkas, O.; Malick, D. K.; Rabuck, A. D.; Raghavachari, K.; Foresman, J. B.; Ortiz, J. V.; Cui, Q.; Baboul, A. G.; Clifford, S.; Cioslowski, J.; Stefanov, B. B.; Liu, G.; Liashenko, A.; Piskorz, P.; Komaromi, I.; Martin, R. L.; Fox, D. J.; Keith, T.; Al-Laham, M. A.; Peng, C. Y.; Nanayakkara, A.; Challacombe, M.; Gill, P. M. W.; Johnson, B.; Chen, W.; Wong, M. W.; Gonzalez, C.; Pople, J. A. *Gaussian 03*; Gaussian, Inc.: Wallingford CT, 2004.

(17) Schaftenaar, G.; Noordik, J. H. *J. Comput.-Aided Mol. Des.* **2000**, *14*, 123.

(18) This is done to keep the Coulomb stabilization of the S−S σ^* orbital constant and to attempt to represent the effect a disulfide linkage in a peptide would experience in the presence of a protonated side chain whose charge center is geometrically constrained.

(19) Our basis of 1s and 1p extra diffuse functions limits us to only the ground and three excited states.

(20) It is difficult to see this barrier in Figure 5. We determined it when we carried out calculations using a much more tightly focused set of R-values in the region of the surface crossing as part of our evaluation of the $H_{1,2}$ matrix element.